EUROPEAN ORGANISATION FOR NUCLEAR RESEARCH

CERN-PPE/92-186
30 October 1992

A Precise Measurement of the τ Lepton Lifetime

The ALEPH Collaboration[‡]

Abstract

Three different techniques are used to measure the mean decay length of the τ lepton with a high precision vertex detector in a sample of 11 800 τ pairs coming from Z decays, collected in 1991 by ALEPH at LEP. Events in which both τ's decay into one charged track are analyzed using two largely independent methods. Displaced vertices in three-prong decays yield another independent measurement. The derived lifetime is $295.5 \pm 5.9 \pm 3.1$ fs, using $m_\tau = 1777.1 \pm 0.5\,\mathrm{MeV}/c^2$. Including previous (1989–1990) ALEPH measurements, the combined τ lifetime is $294.7 \pm 5.4 \pm 3.0$ fs.

(Submitted to Physics Letters B)

[‡]See the following pages for the list of authors.

The ALEPH Collaboration

D. Buskulic, D. Decamp, C. Goy, J.-P. Lees, M.-N. Minard, B. Mours

Laboratoire de Physique des Particules (LAPP), IN^{2}P^3-CNRS, 74019 Annecy-le-Vieux Cedex, France

R. Alemany, F. Ariztizabal, P. Comas, J.M. Crespo, M. Delfino, E. Fernandez, V. Gaitan, Ll. Garrido, T. Mattison, A. Pacheco, C. Padilla, A. Pascual

Institut de Fisica d'Altes Energies, Universitat Autonoma de Barcelona, 08193 Bellaterra (Barcelona), Spain[7]

D. Creanza, M. de Palma, A. Farilla, G. Iaselli, G. Maggi, M. Maggi, S. Natali, S. Nuzzo, M. Quattromini, A. Ranieri, G. Raso, F. Romano, F. Ruggieri, G. Selvaggi, L. Silvestris, P. Tempesta, G. Zito

INFN Sezione di Bari e Dipartimento di Fisica dell' Università, 70126 Bari, Italy

H. Hu,[20] D. Huang, X. Huang, J. Lin, J. Lou, C. Qiao,[20] T. Wang, Y. Xie, D. Xu, R. Xu, J. Zhang, W. Zhao

Institute of High-Energy Physics, Academia Sinica, Beijing, The People's Republic of China[8]

L.A.T. Bauerdick,[24] E. Blucher, G. Bonvicini, F. Bossi, J. Boudreau, D. Casper, H. Drevermann, R.W. Forty, G. Ganis, C. Gay, R. Hagelberg, J. Harvey, S. Haywood, J. Hilgart, R. Jacobsen, B. Jost, J. Knobloch, E. Lançon, I. Lehraus, T. Lohse,[32] A. Lusiani, M. Martinez, P. Mato, H. Meinhard, A. Minten, R. Miquel, H.-G. Moser, P. Palazzi, J.A. Perlas, J.-F. Pusztaszeri,[30] F. Ranjard, G. Redlinger,[25] L. Rolandi, J. Rothberg,[2] T. Ruan,[20,27] M. Saich, D. Schlatter, M. Schmelling, F. Sefkow, W. Tejessy, H. Wachsmuth, W. Wiedenmann, T. Wildish, W. Witzeling, J. Wotschack

European Laboratory for Particle Physics (CERN), 1211 Geneva 23, Switzerland

Z. Ajaltouni, F. Badaud, M. Bardadin-Otwinowska, A.M. Bencheikh, R. El Fellous, A. Falvard, P. Gay, C. Guicheney, P. Henrard, J. Jousset, B. Michel, J-C. Montret, D. Pallin, P. Perret, B. Pietrzyk, J. Proriol, F. Prulhière, G. Stimpfl

Laboratoire de Physique Corpusculaire, Université Blaise Pascal, IN^{2}P^3-CNRS, Clermont-Ferrand, 63177 Aubière, France

T. Fearnley, J.D. Hansen, J.R. Hansen,[1] P.H. Hansen, R. Møllerud, B.S. Nilsson

Niels Bohr Institute, 2100 Copenhagen, Denmark[9]

I. Efthymiopoulos, A. Kyriakis, E. Simopoulou, A. Vayaki, K. Zachariadou

Nuclear Research Center Demokritos (NRCD), Athens, Greece

J. Badier, A. Blondel, G. Bonneaud, J.C. Brient, G. Fouque, S. Orteu, A. Rosowsky, A. Rougé, M. Rumpf, R. Tanaka, M. Verderi, H. Videau

Laboratoire de Physique Nucléaire et des Hautes Energies, Ecole Polytechnique, IN^{2}P^3-CNRS, 91128 Palaiseau Cedex, France

D.J. Candlin, M.I. Parsons, E. Veitch

Department of Physics, University of Edinburgh, Edinburgh EH9 3JZ, United Kingdom[10]

L. Moneta, G. Parrini

Dipartimento di Fisica, Università di Firenze, INFN Sezione di Firenze, 50125 Firenze, Italy

M. Corden, C. Georgiopoulos, M. Ikeda, J. Lannutti, D. Levinthal,[15] M. Mermikides†, L. Sawyer, S. Wasserbaech

Supercomputer Computations Research Institute and Dept. of Physics, Florida State University, Tallahassee, FL 32306, USA [12,13,14]

A. Antonelli, R. Baldini, G. Bencivenni, G. Bologna,[4] P. Campana, G. Capon, F. Cerutti, V. Chiarella, B. D'Ettorre-Piazzoli,[26] G. Felici, P. Laurelli, G. Mannocchi,[5] F. Murtas, G.P. Murtas, L. Passalacqua, M. Pepe-Altarelli, P. Picchi[4]

Laboratori Nazionali dell'INFN (LNF-INFN), 00044 Frascati, Italy

B. Altoon, O. Boyle, P. Colrain, I. ten Have, J.G. Lynch, W. Maitland, W.T. Morton, C. Raine, J.M. Scarr, K. Smith, A.S. Thompson, R.M. Turnbull

Department of Physics and Astronomy, University of Glasgow, Glasgow G12 8QQ,United Kingdom[10]

B. Brandl, O. Braun, C. Geweniger, P. Hanke, V. Hepp, E.E. Kluge, Y. Maumary, A. Putzer, B. Rensch, A. Stahl, K. Tittel, M. Wunsch

Institut für Hochenergiephysik, Universität Heidelberg, 6900 Heidelberg, Fed. Rep. of Germany[16]

A.T. Belk, R. Beuselinck, D.M. Binnie, W. Cameron, M. Cattaneo, D.J. Colling, P.J. Dornan, S. Dugeay, A.M. Greene, J.F. Hassard, N.M. Lieske, J. Nash, S.J. Patton, D.G. Payne, M.J. Phillips, J.K. Sedgbeer, I.R. Tomalin, A.G. Wright

Department of Physics, Imperial College, London SW7 2BZ, United Kingdom[10]

E. Kneringer, D. Kuhn, G. Rudolph

Institut für Experimentalphysik, Universität Innsbruck, 6020 Innsbruck, Austria[18]

C.K. Bowdery, T.J. Brodbeck, A.J. Finch, F. Foster, G. Hughes, D. Jackson, N.R. Keemer, M. Nuttall, A. Patel, T. Sloan, S.W. Snow, E.P. Whelan

Department of Physics, University of Lancaster, Lancaster LA1 4YB, United Kingdom[10]

K. Kleinknecht, J. Raab, B. Renk, H.-G. Sander, H. Schmidt, F. Steeg, S.M. Walther, B. Wolf

Institut für Physik, Universität Mainz, 6500 Mainz, Fed. Rep. of Germany[16]

J-J. Aubert, C. Benchouk, A. Bonissent, J. Carr, P. Coyle, J. Drinkard, F. Etienne, S. Papalexiou, P. Payre, Z. Qian, L. Roos, D. Rousseau, P. Schwemling, M. Talby

Centre de Physique des Particules, Faculté des Sciences de Luminy, IN^{2}P^3-CNRS, 13288 Marseille, France

S. Adlung, C. Bauer, W. Blum,[1] D. Brown, P. Cattaneo,[31] G. Cowan, B. Dehning, H. Dietl, F. Dydak,[23] M. Fernandez-Bosman, M. Frank, A.W. Halley, J. Lauber, G. Lütjens, G. Lutz, W. Männer, R. Richter, H. Rotscheidt, J. Schröder, A.S. Schwarz, R. Settles, H. Seywerd, U. Stierlin, U. Stiegler, R. St. Denis, M. Takashima,[3] J. Thomas,[3] G. Wolf

Max-Planck-Institut für Physik, Werner-Heisenberg-Institut, 8000 München, Fed. Rep. of Germany[16]

J. Boucrot, O. Callot, A. Cordier, M. Davier, J.-F. Grivaz, Ph. Heusse, D.E. Jaffe, P. Janot, D.W. Kim,[19] F. Le Diberder, J. Lefrançois, A.-M. Lutz, M.-H. Schune, J.-J. Veillet, I. Videau, Z. Zhang,

Laboratoire de l'Accélérateur Linéaire, Université de Paris-Sud, IN^{2}P^3-CNRS, 91405 Orsay Cedex, France

D. Abbaneo, S.R. Amendolia, G. Bagliesi, G. Batignani, L. Bosisio, U. Bottigli, C. Bozzi, C. Bradaschia, M. Carpinelli, M.A. Ciocci, R. Dell'Orso, I. Ferrante, F. Fidecaro, L. Foà, E. Focardi, F. Forti, A. Giassi, M.A. Giorgi, F. Ligabue, E.B. Mannelli, P.S. Marrocchesi, A. Messineo, F. Palla, G. Rizzo, G. Sanguinetti, P. Spagnolo, J. Steinberger, R. Tenchini, G. Tonelli, G. Triggiani, C. Vannini, A. Venturi, P.G. Verdini, J. Walsh

Dipartimento di Fisica dell'Università, INFN Sezione di Pisa, e Scuola Normale Superiore, 56010 Pisa, Italy

J.M. Carter, M.G. Green, P.V. March, Ll.M. Mir, T. Medcalf, I.S. Quazi, J.A. Strong, L.R. West

Department of Physics, Royal Holloway & Bedford New College, University of London, Surrey TW20 OEX, United Kingdom[10]

D.R. Botterill, R.W. Clifft, T.R. Edgecock, M. Edwards, S.M. Fisher, T.J. Jones, P.R. Norton, D.P. Salmon, J.C. Thompson

Particle Physics Dept., Rutherford Appleton Laboratory, Chilton, Didcot, Oxon OX11 OQX, United Kingdom[10]

B. Bloch-Devaux, P. Colas, H. Duarte, W. Kozanecki, M.C. Lemaire, E. Locci, S. Loucatos, E. Monnier, P. Perez, F. Perrier, J. Rander, J.-F. Renardy, A. Roussarie, J.-P. Schuller, J. Schwindling, D. Si Mohand, B. Vallage

Service de Physique des Particules, DAPNIA, CE-Saclay, 91191 Gif-sur-Yvette Cedex, France[17]

R.P. Johnson, A.M. Litke, G. Taylor, J. Wear

Institute for Particle Physics, University of California at Santa Cruz, Santa Cruz, CA 95064, USA[29]

J.G. Ashman, W. Babbage, C.N. Booth, C. Buttar, R.E. Carney, S. Cartwright, F. Combley, F. Hatfield, P. Reeves, L.F. Thompson[1]

Department of Physics, University of Sheffield, Sheffield S3 7RH, United Kingdom[10]

E. Barberio, A. Böhrer, S. Brandt, C. Grupen, F. Rivera, U. Schäfer

Fachbereich Physik, Universität Siegen, 5900 Siegen, Fed. Rep. of Germany[16]

G. Giannini, B. Gobbo, F. Ragusa[22]

Dipartimento di Fisica, Università di Trieste e INFN Sezione di Trieste, 34127 Trieste, Italy

L. Bellantoni, W. Chen, D. Cinabro,[28] J.S. Conway, D.F. Cowen,[21] Z. Feng, D.P.S. Ferguson, Y.S. Gao, J. Grahl, J.L. Harton, R.C. Jared,[6] B.W. LeClaire, C. Lishka, Y.B. Pan, J.R. Pater, Y. Saadi, V. Sharma, M. Schmitt, Z.H. Shi, A.M. Walsh, F.V. Weber, M.H. Whitney, Sau Lan Wu, X. Wu, G. Zobernig

Department of Physics, University of Wisconsin, Madison, WI 53706, USA[11]

[†] Deceased.

[1] Now at CERN, PPE Division, 1211 Geneva 23, Switzerland.

[2] Permanent address: University of Washington, Seattle, WA 98195, USA.

[3] Now at SSCL, Dallas, TX, U.S.A.

[4] Also Istituto di Fisica Generale, Università di Torino, Torino, Italy.

[5] Also Istituto di Cosmo-Geofisica del C.N.R., Torino, Italy.

[6] Permanent address: LBL, Berkeley, CA 94720, USA.

[7] Supported by CICYT, Spain.

[8] Supported by the National Science Foundation of China.

[9] Supported by the Danish Natural Science Research Council.

[10] Supported by the UK Science and Engineering Research Council.

[11] Supported by the US Department of Energy, contract DE-AC02-76ER00881.

[12] Supported by the US Department of Energy, contract DE-FG05-87ER40319.

[13] Supported by the NSF, contract PHY-8451274.

[14] Supported by the US Department of Energy, contract DE-FC0S-85ER250000.

[15] Supported by SLOAN fellowship, contract BR 2703.

[16] Supported by the Bundesministerium für Forschung und Technologie, Fed. Rep. of Germany.

[17] Supported by the Direction des Sciences de la Matière, C.E.A.

[18] Supported by Fonds zur Förderung der wissenschaftlichen Forschung, Austria.

[19] Supported by the Korean Science and Engineering Foundation and Ministry of Education.

[20] Supported by the World Laboratory.

[21] Now at California Institute of Technology, Pasadena, CA 91125, USA.

[22] Now at Dipartimento di Fisica, Università di Milano, Milano, Italy.

[23] Also at CERN, PPE Division, 1211 Geneva 23, Switzerland.

[24] Now at DESY, Hamburg, Germany.

[25] Now at TRIUMF, Vancouver, B.C., Canada.

[26] Also at Università di Napoli, Dipartimento di Scienze Fisiche, Napoli, Italy.

[27] On leave of absence from IHEP, Beijing, The People's Republic of China.

[28] Now at Harvard University, Cambridge, MA 02138, U.S.A.

[29] Supported by the US Department of Energy, grant DE-FG03-92ER40689.

[30] Visitor from University of Wisconsin, Madison, WI 53706, USA.

[31] Now at Università di Pavia, Pavia, Italy.

[32] Now at Max-Planck-Institut f. Kernphysik, Heidelberg, Germany.

1 Introduction

The study of weak interactions has led to the formulation of a lepton universality principle stating that amplitudes of charged current processes do not depend on lepton generation. Measurements of τ lepton properties are less precise than those achieved for μ and e. In particular, experimental information on charged current interactions of the τ is available only through measurements of its decays. Comparing the decay rates for $\tau \rightarrow e\overline{\nu}_e\nu_\tau$ and $\mu \rightarrow e\overline{\nu}_e\nu_\mu$ tests μ-τ universality:

$$\left(\frac{g_\tau}{g_\mu}\right)^2 = \left(\frac{m_\mu}{m_\tau}\right)^5 \frac{\tau_\mu}{\tau_\tau} B(\tau \rightarrow e\overline{\nu}_e\nu_\tau). \quad (1)$$

The g_l are the strengths of the charged current couplings, m_l and τ_l are the masses and lifetimes of τ and μ, and $B(\tau \rightarrow e\overline{\nu}_e\nu_\tau)$ is the electron branching fraction of the τ lepton. Using the published values of m_τ [1] and $B(\tau \rightarrow e\overline{\nu}_e\nu_\tau)$ [1], and the average τ lifetime [2–14], an apparent deviation from universality at the 2σ level was observed: $g_\tau/g_\mu = 0.973 \pm 0.012$. Possible explanations for such a deviation are listed in [15]. Recent measurements of the τ mass [16, 17] yield a revised world average of $1777.1 \pm 0.5\,\mathrm{MeV}/c^2$ and a smaller deviation from universality.

At LEP the high purity of the τ sample and the reduced multiple scattering due to high track momentum provide favourable experimental conditions for this lifetime measurement [10–13]. In this paper a τ lifetime measurement is presented which takes advantage of the greatly improved impact parameter resolution achieved with the new silicon strip vertex detector installed in ALEPH before the 1991 data taking period.

This letter describes three analysis methods: first a new technique based on the distance between tracks at the production point in 1-1 topology events, then the impact parameter difference analysis introduced in a previous letter [13], and finally the conventional analysis of the decay length for τ decaying into three prongs.

2 Experimental Setup and Data Sample

The configuration of the ALEPH detector is described in detail elsewhere [18]. Two relevant changes were performed before the 1991 data taking period. The 7.8 cm radius aluminium beam pipe was replaced by a 5.3 cm beryllium one. A high resolution vertex detector (VDET) consisting of two layers of 300 μm thick silicon wafers was inserted [19]. Each layer provides measurements both in the r-ϕ and r-z views at average radii of 6.3 and 10.8 cm. The spatial resolution for the r-ϕ coordinate is 12 μm and varies between 12 and 22 μm for the z coordinate, depending on track polar angle. The solid angle coverage is 85% for the inner layer and 69% for the outer layer.

The design of the VDET includes a 5% overlap between the active regions of wafers adjacent in r-ϕ. Using tracks which go through this region the relative position of adjacent wafers is measured with an accuracy of less than 2 μm. Forcing agreement around the full circumference gives a statistical error of about 1 μm on the average radial position of the

wafers. Using the global alignment procedure the radial positions of the individual detectors are known to a precision of 5 μm (rms) over the full active area. Thus, the fractional error on decay length coming from a systematic error in the average radial position of VDET wafers is less than 10^{-4}.

Charged particles, once outside VDET, cross the inner tracking chamber (ITC) and the time projection chamber (TPC). The ITC is a cylindrical drift chamber with eight axial wire layers at radii of 16 to 26 cm. The TPC provides up to 21 space points per track at radii between 40 and 171 cm. Tracking is performed in a 1.5 T magnetic field.

Detector-induced distortions in the measurement of impact parameter d could lead to biases in d which depend on ϕ, θ, etc. In the case that the detector has no dead zones in ϕ, these distortions do not cause a first order change in the measured decay length in the r-ϕ plane. However, correlated offsets in d and ϕ would introduce a second order decay length bias. From a study of $Z \to \mu^+\mu^-$ and $q\bar{q}$ events, the size of this effect is found to be less than 2 μm or 0.1% of the mean τ decay length.

The electromagnetic calorimeter (ECAL) is used in this analysis to reject Bhabha events and to identify $e^{\pm}$ tracks which have undergone hard bremsstrahlung in the detector material. It is also used to measure photons and to remove $\tau^+\tau^-$ events accompanied by final state radiation. The ECAL is a lead/wire-chamber sandwich operated in proportional mode. The calorimeter is read out via projective towers subtending typically 15 mrad $\times$ 15 mrad in solid angle which sum the deposited energy in three sections in depth. The high granularity of the ECAL is particularly suited to τ physics at LEP, where τ's decay into narrow jets. The energy resolution for photons and electrons is $\sigma_E/E \sim 0.2/\sqrt{E}$ and a typical angular precision of $\sim 3.5\,\mathrm{mrad}/\sqrt{E}$ is achieved.

The hadron calorimeter (HCAL) uses the iron return yoke as absorber with an average depth of 1.50 m. Hadronic showers are sampled by 23 planes of streamer tubes, providing a digital hit pattern and inducing an analog signal on pads arranged in projective towers. The HCAL is used in combination with two layers of muon chambers outside the magnet for μ identification.

Charged particle tracks are reconstructed in the VDET-ITC-TPC system. The fit to the measured coordinates takes into account coordinate resolution and multiple scattering effects. An impact parameter resolution of 28 μm is achieved in the r-ϕ plane for muons from $Z \to \mu^+\mu^-$ having at least one VDET r-ϕ hit [20]. With the help of VDET the beam position is determined with a precision of 30 μm horizontally and 10 μm vertically, averaged over blocks of about 100 hadronic events. Measurement of the effective size of the interaction region gives $\sigma_x = 142 \pm 2\,\mu$m, $\sigma_y \lesssim 8\,\mu$m, $\sigma_z = 0.93 \pm 0.01$ cm, averaged over the whole data sample.

Energy releases in ECAL and HCAL are reconstructed separately. Electromagnetic clusters are considered photon candidates if their distance from the impact point of a charged track is greater than 4 cm [21]. A procedure that combines information from charged and neutral particles is applied to determine the flow of energy in the event [22].

The data sample used in this analysis was collected in 1991 at centre-of-mass energies between 88.5 and 93.7 GeV. Data with fully functional tracking detectors represent an integrated luminosity of $10.3\,\mathrm{pb}^{-1}$ or about 11 800 produced τ pair events. The τ pair

selection procedure is described in detail in [23] and so only a brief account is given here. Hadronic Z decays are rejected by selecting events with more than one and less than seven charged tracks forming well collimated back-to-back jets compatible with τ decays. Electron and muon pairs are removed by requiring a mass-squared recoiling against the two track system greater than $400\,(\mathrm{GeV}/c^2)^2$. A further cut against electron pairs is applied, asking less than 55 GeV deposited in the ECAL. The overall efficiency for this selection is 73%, with a total background contribution from other Z decays and two-photon interactions of 3%. The $\tau^+\tau^-$ sample contains 8896 candidate events to which further cuts are applied for the different analyses.

3 Analysis of One-Prong τ Decays

For a τ decaying into a single charged particle one can in principle determine the decay length from the decay angle and the impact parameter of the track with respect to the production point. In practice, however, if one considers a single τ decay in e^+e^- collisions such a procedure is not applicable: the production point is known only with the precision of the beam size and the τ direction cannot be precisely measured because of undetected neutrinos in the decay. To recover most of the missing information from 1-1 topology events (74% of all τ pairs) the two methods described herein use the information provided by both τ decays. It is needed in this case to assume that the τ's are produced back-to-back. This is achieved by working in the r-ϕ projection which does not suffer from acollinearity caused by initial state radiation and by vetoing large angle final state radiation as explained below.

The first approach (Impact Parameter Sum) aims to measure the distance between the tracks at their point of closest approach to the beam axis. This is an effective application of the vertex detector, cancelling smearing in the reconstructed impact parameter d from the beam size which would otherwise dominate the resolution. The following convention is used to choose the sign of d: d is positive if the particle moves counterclockwise in the r-ϕ plane with respect to the beam axis when at minimum distance. Then $\delta = d_1 + d_2$ does not depend on the Z production point (see fig. 1). This is strictly true only if the tracks are collinear, otherwise a contribution proportional to their acollinearity and to the beam size appears. The event sphericity axis, computed with charged and neutral particles, is used to estimate the τ direction. For a fixed pair of decay angles (ψ'_1, ψ'_2), each d_i has an exponential distribution with mean $\ell \sin\theta \sin\psi'_i$, where ℓ is the average decay length and θ is the τ polar angle. The distribution of δ is a combination of these two exponential functions which depends on the magnitudes and relative signs of the decay angles ψ'_1 and ψ'_2. A maximum likelihood fit for ℓ is then performed, accounting for the errors on δ and $\psi'_{1,2}$.

The second method (Impact Parameter Difference), described in detail in [13], eliminates the need to estimate the τ direction by considering the azimuthal angle between the two daughter tracks and the algebraic difference of their impact parameters. The lifetime is determined from the measured correlation between these quantities. The result is insensitive to assumptions on detector resolution and decay angular distributions. The beam size contributes doubly to the smearing on the impact parameter difference, reducing the statistical precision of the measurement.

In both of these methods, the statistical error on the τ decay length is increased by smearing from measurement errors. The largest contributions to the statistical uncertainties in the two analyses are the τ direction uncertainty and the beam size, respectively. The measurements therefore have nearly independent statistical errors, although the samples used overlap to a large extent.

4 Impact Parameter Sum Analysis

4.1 Likelihood Function

For the configuration shown in fig. 1a, where the true angles ψ_1' and ψ_2' are positive, the distribution of the true sum of impact parameters δ' is given by

$$\frac{dN}{d\delta'} = \begin{cases} \dfrac{\exp\left(-\delta'/\ell\sin\theta\sin\psi_1'\right) - \exp\left(-\delta'/\ell\sin\theta\sin\psi_2'\right)}{\ell\sin\theta(\sin\psi_1' - \sin\psi_2')} & \delta' > 0 \\ 0 & \delta' < 0 \end{cases} \qquad \psi_1' > 0, \psi_2' > 0. \quad (2)$$

This is obtained by folding the exponentials for d_1 and d_2, imposing $\delta' = d_1 + d_2$. On the other hand if $\psi_1' > 0$, $\psi_2' < 0$ as in fig. 1b, the distribution is

$$\frac{dN}{d\delta'} = \begin{cases} \dfrac{\exp\left(-\delta'/\ell\sin\theta\sin\psi_1'\right)}{\ell\sin\theta(\sin\psi_1' - \sin\psi_2')} & \delta' > 0 \\ \dfrac{\exp\left(-\delta'/\ell\sin\theta\sin\psi_2'\right)}{\ell\sin\theta(\sin\psi_1' - \sin\psi_2')} & \delta' < 0 \end{cases} \qquad \psi_1' > 0, \psi_2' < 0. \quad (3)$$

The expectation value of the distributions in eqs. 2 and 3 is always $\ell\sin\theta\,(\sin\psi_1' + \sin\psi_2')$.

The distribution for the observed sum of impact parameters δ is obtained by convolving the true δ' distribution with a resolution function for δ and the observed angles ψ_1 and ψ_2. Since the angular error contribution from tracking ($\simeq 0.5\,\mathrm{mrad}$) is negligible with respect to the sphericity axis fluctuations ($\simeq 20\,\mathrm{mrad}$), the resolution function can be factored into two independent functions g and h:

$$\frac{dN(\delta,\psi_1,\psi_2)}{d\delta} = \int d\psi_1'\, d\psi_2'\, h(\psi_1,\psi_2,\psi_1',\psi_2') \int d\delta'\, g(\delta,\delta')\, \frac{dN(\delta',\psi_1',\psi_2')}{d\delta'}. \quad (4)$$

The smearing on δ, characterized by the function g, is dominated by the resolution of the tracking devices, and in particular of the VDET. The tracking errors on δ are described by a Gaussian distribution with variance σ_t^2, as discussed in section 4.3. As mentioned above an additional smearing on δ comes from the size of the beam. This small contribution is modelled by a Gaussian function with variance

$$\sigma_b^2 = 4\sin^2\frac{\Delta\phi}{2}\,(\sigma_x^2\sin^2\overline{\phi} + \sigma_y^2\cos^2\overline{\phi}), \quad (5)$$

where σ_x and σ_y describe the beam size, $\overline{\phi} = (\phi_1 + \phi_2)/2$ is the average of the track azimuthal angles and $\Delta\phi = \phi_1 - \phi_2 \pm \pi$ is the acollinearity of the tracks in the r-ϕ projection. The errors σ_t and σ_b are computed for each event.

Fluctuations in the decay angles come from approximating the unknown τ direction with the sphericity axis of the event. Event axis errors depend primarily on the momentum and direction of the undetected neutrinos, the detector resolution playing only a marginal role. The resolution function h gives the probability for a pair with original angles (ψ'_1, ψ'_2) to have the measured values (ψ_1, ψ_2). This function depends on the decay properties of the τ and is obtained by determining the sphericity axis on a high statistics sample of Monte Carlo τ pairs without full detector simulation. It should be noted that in practice the deviation of $S = \psi_1 + \psi_2$ from $S' = \psi'_1 + \psi'_2$ is studied as a function of S and $D = \psi_1 - \psi_2$. Neglecting ψ measurement errors and the τ's acollinearity, it is assumed that $\psi'_1 - \psi'_2 = \psi_1 - \psi_2$. The distributions of S and D for data and Monte Carlo are shown in fig. 2. By comparing the S and S' distributions in Monte Carlo (fig. 2a), one can see the systematic narrowing of S caused by errors in the event axis determination[1]

The likelihood of each event is obtained by performing the integrations of eq. 4. The convolution of $\frac{dN}{d\delta'}$ with g can be expressed analytically. A numerical integration on S' is then performed, care being taken to pick up the correct expression according to the signs of ψ'_1, ψ'_2, and δ. The global likelihood is maximized with respect to the mean decay length ℓ.

4.2 Event Selection

Starting from the sample of candidate τ pairs, cuts are applied to select the 1-1 configurations which contain well measured tracks, that is, with a sufficient number of points in the TPC and ITC and at least one r-ϕ hit in the VDET (table 1). The loss of events at this point comes mainly from the limited solid angle subtended by the vertex detector. To reduce the lifetime bias due to nuclear interactions in the detector material a stringent cut on events containing extra charged tracks is used. Events containing isolated photons are rejected: the invariant mass of any photon and the nearest charged track must be less than 2 GeV/c^2. This requirement is designed to remove $\tau^+\tau^-$ events with final state radiation. Electrons undergoing hard bremsstrahlung in the detector material suffer appreciable variations in the reconstructed ϕ and d. When an electron and a close photon are identified, the event is rejected if the variation $|\Delta d|$ estimated from the ECAL information and the $e^{\pm}$ momentum is greater than 100 μm [13]. Finally, the requirement $|\psi_i| < 150$ mrad is imposed to further reduce the background from $\gamma\gamma$ processes. The resulting distribution of δ is shown in fig. 3a. The solid histogram represents the Monte Carlo sample used in the analysis [24], normalized to the data, the points are the τ data, and the hatched histogram comes from a simulated zero-lifetime τ sample. The δ resolution obtained from Monte Carlo is 76 μm (rms), giving full access to the lifetime information. For comparison the analogous distribution for dimuons from Z decays is shown in fig. 3b.

[1]The sphericity axis is used rather than the thrust axis to estimate the τ direction because it results in a smaller distortion of the S distribution.

Table 1: Numbers of surviving candidates in the impact parameter sum analysis.

Cut	Events
1-1 topology	5574
Bhabha rejection	5483
$\sum q = 0$	5336
No extra track	4713
$p > 1\,\mathrm{GeV}/c$	4570
$N_{TPC} \geq 9$	4538
$N^1_{ITC} + N^2_{ITC} \geq 12$	4189
$N_{VDET} \geq 1$	3086
$\sum \chi^2/\mathrm{D.o.f.} < 7$	3017
Isolated γ rejection	2827
Bremsstrahlung rejection	2572
$\lvert\psi\rvert < 0.15$ rad	2480
$\lvert\delta\rvert < 0.18\,\mathrm{cm}$	2479

4.3 Fit Results on Monte Carlo and Data

The likelihood function described previously contains a Gaussian with standard deviation σ_t coming from tracking performance. Though the helix fit procedure provides the errors (σ_1, σ_2) on the two impact parameters, a calibration of errors with data is necessary due to imperfections in the model. To correct the calculated errors from coordinate measurement and multiple scattering, and to account for residual misalignments, the form $\sigma_t^2 = \kappa^2(\sigma_1^2 + \sigma_2^2) + \rho^2$ is adopted for the tracking error on δ. The importance of these effects varies with track momentum. In order to cover the full momentum range an analysis of dimuon events produced in Z decays and in $\gamma\gamma$ collisions is used to determine the values $\kappa^2 = 1.14 \pm 0.15$ and $\rho^2 = 490 \pm 140\,\mu\mathrm{m}^2$ with a -97% error correlation. Using these values, the fit to the data gives a mean decay length $\ell = 0.2125 \pm 0.0055\,\mathrm{cm}$. The systematic uncertainty from the parametrization of σ_t is $0.0022\,\mathrm{cm}$. Figures 4a–e show the distribution of δ divided in bins of $\psi_1 + \psi_2$. Superimposed on the data is the best fit distribution.

Biases are expected due to the approximations in the evaluation of h, in particular due to the the binning of h. This bias is determined from fully simulated τ events, fitted with the same procedure (figs. 4f–j). An analysis of the residuals over the whole momentum range in simulated τ events gives $\kappa^2 = 1.30 \pm 0.02$, setting $\rho^2 = 0$. The choice $\rho^2 = 0$ was found to be consistent with the absence of variation of κ with momentum in Monte Carlo events. The fitted τ decay length in Monte Carlo is $\ell = 0.2262 \pm 0.0025\,\mathrm{cm}$, to be compared with the expected value of $0.2328\,\mathrm{cm}$ for a lifetime of 304 fs, a mass of $1777.1\,\mathrm{MeV}/c^2$, and a centre of mass energy of $91.20\,\mathrm{GeV}$, including radiative corrections to the τ momentum. The decay length bias introduced by the reconstruction and fitting procedure is thus found to be $-2.8 \pm 1.1\%$.

The following sources of background are considered: $\mathrm{Z} \to \mathrm{q\bar{q}}$, $\mathrm{e^+e^-}$, and $\mu^+\mu^-$; $\gamma\gamma \to l^+l^-$ where $l = \mathrm{e}, \mu, \tau$; and $\gamma\gamma \to$ hadrons. Hadronic background is negligible in the 1-1 sample. The contamination from the other channels is predicted by Monte Carlo to be $2.5 \pm 0.3\%$, leading to a lifetime bias of $-0.6 \pm 0.4\%$.

Table 2: Systematic biases and uncertainties in the impact parameter sum analysis.

	$\Delta\tau_\tau/\tau_\tau$ (%)
Bias in Monte Carlo	-2.8 ± 1.1
σ_t Parametrization	± 0.9
Background	-0.6 ± 0.4
τ Branching Ratios	± 0.8
τ Transverse Polarization	-0.5 ± 0.5
Beam Size	negligible
Total	-3.9 ± 1.8

Other biases originate in the simulation of the event axis uncertainty. Two aspects of the τ decay simulation which affect the event axis determination are the branching ratios and the correlation of the τ^+ and τ^- transverse polarizations. Branching ratios for the various one-prong modes are varied within their errors [25], yielding a lifetime uncertainty of $\pm 0.8\%$. Transverse polarization correlation effects, which are not simulated in KORALZ [24], are studied using the generator KORALB[2] [26]. These effects would correlate the decay angles of the two τ's in the r-ϕ projection, therefore influencing the event axis error. Events are generated with and without the correlation. The fitted decay length is found to be $0.5 \pm 0.5\%$ smaller when the correlation is included. A correction is applied for this bias in the Monte Carlo calibration sample.

The systematic biases and uncertainties are summarized in table 2. Correcting the measured decay length for the biases and assuming a τ mass of $1777.1\,\mathrm{MeV}/c^2$ yields

$$\tau_\tau = 288.3 \pm 7.5\,(\mathrm{stat}) \pm 5.1\,(\mathrm{syst})\,\mathrm{fs}$$

for this analysis.

5 Impact Parameter Difference Analysis

The 1-1 topology events were also analyzed with the impact parameter difference method. This method is based on the fact that (1) the τ^+ and τ^- are produced nearly back-to-back in the r-ϕ projection and (2) $\sin\psi \cong \psi$. The mean difference of impact parameters (for fixed angles) is given by $\langle d_+ - d_- \rangle = \ell(\sin\psi_+ - \sin\psi_-)\sin\theta \cong \ell\Delta\phi\sin\theta$. The full details of this procedure are given in [13].

The following quantities are determined for each event:

$$\begin{aligned} Y &= d_+ - d_-, \\ X &= \frac{\bar{p}_\tau(\sqrt{s})}{\bar{p}_\tau(\mathrm{peak})}\,\Delta\phi\,\sin\theta, \end{aligned}$$

where $\bar{p}_\tau(\sqrt{s})$ is the mean τ momentum, determined from Monte Carlo simulation after all event selection criteria are applied, and θ is taken from the event thrust axis. No estimate of

[2]The version of this program used has Z exchange, however it is not appropriate for general studies as it lacks radiative corrections.

Table 3: Numbers of surviving candidates in the impact parameter difference analysis.

Cut	Events
1-1 topology, $\sum q = 0$	5536
No extra track, $2 < \|d\| < 40\,\text{cm}$	5223
Cosmic ray rejection	5217
$N_{VDET} \geq 1$	4035
$N_{ITC} \geq 4$	3973
χ^2/D.o.f. < 5	3848
$p > 1\,\text{GeV}/c$	3733
Bremsstrahlung rejection	3407
Isolated γ rejection	3237
$\|X\| < 0.18$	3205

the τ direction is needed to determine $\Delta\phi$. The lifetime is then determined from the Y *vs.* X distribution and the relation

$$\langle Y \rangle = \left[\frac{\bar{p}_\tau(\text{peak})}{m_\tau} \tau_\tau \right] X. \tag{6}$$

The quantity in brackets corresponds to the slope of $\langle Y \rangle$ *vs.* X and is equal to the mean τ laboratory decay length at the reference "peak" energy of $\sqrt{s} = 91.25\,\text{GeV}$.

The essential difference with the analysis described in [13] is the additional requirement of at least one VDET r-ϕ hit associated with each track (table 3). Besides improving the d resolution, this requirement provides powerful rejection of mismeasured tracks, including those undergoing hard scattering or bremsstrahlung in the ITC or TPC. Several other refinements have been made in the event selection to reduce systematic errors. Events containing one or more extra charged tracks not emanating from the interaction point ($2\,\text{cm} < |d| < 40\,\text{cm}$) are rejected. This reduces the lifetime bias due to nuclear interactions in the detector material. The more stringent requirement $|\Delta d| < 100\,\mu\text{m}$ is now used with the bremsstrahlung rejection procedure. Finally, better rejection of $\gamma\tau^+\tau^-$ events is achieved by considering photons down to 1 GeV energy and by requiring a γ–charged-track invariant mass below $2\,\text{GeV}/c^2$. There are 3205 events remaining with $|X| < 0.18$.

The Y *vs.* X distribution is shown in fig. 5a. The parameters of the line $Y = a_0 + a_1 X$ are obtained from the data with an unbinned least-squares fit. To reduce the statistical uncertainty on the fitted slope, each event i is weighted by $1/\sigma^2(Y_i)$; the $\sigma(Y_i)$ account for tracking errors and smearing due to the beam size and the exponential decay time distribution. In order to reduce fluctuations and biases caused by poorly measured tracks, an iterative trimming procedure is employed. After each iteration, the fitted values of a_0 and a_1 are used to compute the residual $\Delta_i = Y_i - a_0 - a_1 X$ for each event. Events with $|\Delta_i| < \Delta_{\text{trim}}$ are considered in the next iteration. A value of $690\,\mu\text{m}$ is chosen for Δ_{trim}, removing approximately 1% of the events from each tail. The fit results are $a_0 = +0.0002 \pm 0.0004\,\text{cm}$ and $a_1 = +0.2196 \pm 0.0084\,\text{cm}$, with $\chi^2 = 2777$ for 3139 degrees of freedom (fig. 5b). The statistical uncertainty on a_1 is independently calculated by fitting many random samples of $\{Y_i\}$ which are generated from the observed distribution of Δ_i/σ_i. The uncertainty so

Table 4: Systematic biases and uncertainties in the impact parameter difference analysis.

	$\Delta\tau_\tau/\tau_\tau$ (%)
Selection Bias	-0.5 ± 0.4
$\Delta\phi \cong \sin\psi_+ - \sin\psi_-$ Approximation	-0.2 ± 0.0
τ Acollinearity	-0.2 ± 0.3
Tracking Errors + Trimming	-5.3 ± 0.6
Simulation of Detector Resolution	negligible
Detector Alignment	± 0.1
Simulation of Track Fit χ^2	± 0.2
Backgrounds	-1.5 ± 0.8
Total	-7.6 ± 1.1

obtained, 0.0085 cm, is used in the lifetime determination.[3]

The fitted value of a_1 is corrected for several biases which are estimated from Monte Carlo simulation (table 4). The lifetime bias introduced by the selection procedure is $-0.5 \pm 0.4\%$. The assumption that $\Delta\phi \cong \sin\psi_+ - \sin\psi_-$ results in a bias on a_1 of -0.2%. The acollinearity of the τ pairs in the remaining $\gamma\tau^+\tau^-$ events yields a bias of $-0.2 \pm 0.3\%$. This uncertainty is based on a study of isolated photons in data and Monte Carlo.

The bias due to track measurement errors is $+1.3 \pm 0.5\%$. The trimming procedure removes some well-measured events with long τ lifetimes, introducing a negative bias on a_1 of $-6.6 \pm 0.6\%$. The statistical errors on these two biases are anti-correlated; the net bias due to tracking errors and trimming is $-5.3 \pm 0.6\%$. The systematic uncertainty on the lifetime associated with simulation of the detector resolution is negligible. Comparisons of the numbers of nuclear and bremsstrahlung interactions in data and Monte Carlo indicate that these contributions to the lifetime uncertainty are also negligible. Detector alignment errors yield an uncertainty of $\pm 0.1\%$. The simulation of the number of electrons surviving the track fit χ^2 cut contributes $\pm 0.2\%$ to the lifetime uncertainty. The measured lifetime is insensitive to the size of the interaction region: when the generated σ_x and σ_y are increased by 50% in the Monte Carlo (without changing the values assumed in the fit), the fitted slope changes by $-0.5 \pm 0.6\%$.

The net lifetime bias due to backgrounds is estimated from Monte Carlo simulation to be $-1.5 \pm 0.2\%$, to which an additional systematic uncertainty of $\pm 0.7\%$ is assigned allowing for a 50% uncertainty in the effect of the background. Two-photon interactions are the dominant source of background, amounting to 1.4% of the final sample.

The calculated biases, particularly that due to trimming, depend on the input Monte Carlo τ lifetime. A variation in τ_τ of $\pm 3.9\%$ (corresponding to the statistical uncertainty on a_1) leads to a change in the total bias of $\mp 0.3\%$. This is accounted for in the calculation of τ_τ and its statistical error.

Variations in the fitted slope a_1 are correctly reproduced by the Monte Carlo as the fit limit on $|X|$ is changed to 0.14 or 0.22, and as the effective trim fraction is varied between

[3] If trimming were not performed, the χ^2 would be 4138 for 3203 degrees of freedom, and the statistical uncertainty on a_1 would be 4.0% rather than 3.9%.

0 and 25% in each tail. The measured lifetimes obtained with and without trimming differ by 0.4%; the expected rms difference is 3.0%. The lifetime is also insensitive to variations in the event weight contributions.

Using $\bar{p}_\tau(\text{peak}) = 45.40\,\text{GeV}/c$ and $m_\tau = 1777.1\,\text{MeV}/c^2$ in eq. 6 gives

$$\tau_\tau = 310.5 \pm 13.0\,(\text{stat}) \pm 3.5\,(\text{syst})\,\text{fs}.$$

6 Decay Length Analysis

In the decay length method secondary vertices are reconstructed using the full three-dimensional information provided by the detector; together with the beam position and its size, the τ flight distance is computed. A maximum likelihood fit is then performed to determine the average decay length.

The τ pair sample is the same as that described before. Three-prong τ decays are selected from the τ candidates by requiring three tracks in the same hemisphere with total charge equal to ± 1. To ensure good quality tracking, each track should have at least eight TPC points, and at least two points in the ITC or one in VDET. VDET measurements in both the r-ϕ and r-z views are considered. The track momentum must be larger than $0.3\,\text{GeV}/c$ and the helix fit χ^2 must be less than four times the number of degrees of freedom. The track should come from within 4 cm of the origin in z and have an impact parameter smaller than 0.5 cm. Moreover, at least two tracks are required to have coordinate points in the VDET. The numbers of surviving candidates at various stages of the selection are given in table 5.

In order to reject the remaining hadronic events, three-prong decay candidates are retained only if their invariant mass is less than $1.5\,\text{GeV}/c^2$. Decays with an identified electron are rejected to reduce contamination from photon conversion.

A three-dimensional vertex fit is performed from the track parameters, and the decay candidates are retained only if the vertex χ^2 probability is greater than 4%. This cut rejects 36% of the τ's (27% in Monte Carlo). Most of the rejected candidates have incorrectly assigned VDET hits. The fraction of events showing this pattern recognition problem is not simulated correctly. As shown below, this does not affect appreciably the lifetime measurement.

For each candidate the decay length in space is found using a least-squares procedure similar to the one outlined in [13], searching for the best τ production and decay points around the beam spot and the secondary vertex, respectively, but constraining the τ flight path to be parallel to the sphericity axis. Errors in the τ direction are decoupled from the decay length fit by increasing the assumed beam spot size in the plane orthogonal to the τ direction. This procedure has no effect on the decay length resolution. In the Monte Carlo sample this fit χ^2 probability distribution shows a small excess near zero, due to events with reconstruction problems. These are removed by applying a cut at 1% probability; it was checked that no bias is introduced. An average decay length resolution of $740\,\mu\text{m}$ is achieved in Monte Carlo data. Candidates for which the computed error on the decay length is greater than 0.3 cm are also rejected. Figure 6 shows the decay length distribution for the remaining 909 τ decays.

Table 5: Numbers of surviving candidates in three-prong selection.

Cut	Decays
Three-track jet	2463
Track quality cuts	1882
No electron	1483
Invariant mass $< 1.5\,\mathrm{GeV}/c^2$	1458
Probability of vertex fit > 0.04	930
Probability of decay length fit > 0.01	920
Computed error lower than 0.3 cm	909

The mean decay length is extracted from the decay length distribution using a maximum likelihood method. The probability function is taken as the convolution of a decreasing exponential with a Gaussian resolution function. The decay length uncertainties are multiplied by a scaling factor k which is also extracted from the fit. The mean decay length ℓ is adjusted to correspond to a center of mass energy of 91.25 GeV. The results for data are $\ell = 0.2252 \pm 0.0080\,\mathrm{cm}$ and $k = 1.176 \pm 0.064$; the error on ℓ is dominated by the exponential width. For simulated events, the same procedure gives $\ell = 0.2311 \pm 0.0029\,\mathrm{cm}$ and $k = 1.103 \pm 0.023$. The fitted ℓ is in agreement with the expected value, 0.2329 cm, for $m_\tau = 1777.1\,\mathrm{MeV}/c^2$ and $\tau_\tau = 304\,\mathrm{fs}$. The k value reflects the imperfect assignment of the error by the helix fit program.

Several sources of systematic errors are studied. First, the bias due to the residual contamination of hadronic events is found from Monte Carlo simulation to be $-0.6 \pm 0.3\%$. The contamination from one-prong decays with photon conversions is also studied from Monte Carlo; it is found to have an effect of $\pm 0.2\%$. More important are the effects of pattern recognition errors. Events with problems in track-hit association are expected to be concentrated at low χ^2 probability in the vertex fit. This can be seen by studying how the factor k and the decay length vary when the cut on the vertex χ^2 probability is changed from 0.2 to very small values (fig. 7a,b). One can see that at low χ^2 probability values the factor k grows, showing the presence of tails in the resolution function. For cuts greater than 0.04 the variation can be explained by statistics alone, implying that the contamination from wrong association has been reduced to a constant level. On the other hand, the decay length rises slowly due to the correlation with k and tends toward a constant for vertex probabilities greater than 0.04. A similar behaviour is seen in the data. In fig. 7c the ratio of the data and Monte Carlo decay lengths is shown as a function of the cut on χ^2 probability. To estimate the effect of the possibly different pattern recognition error rates in data and Monte Carlo, the variation of the ratio obtained by changing this cut by ± 0.02 is taken as the systematic uncertainty ($\pm 0.6\%$). As a further check the fitted lifetime was studied as a function of the opening angle of the τ decay products since pattern recognition problems were expected to be linked to small opening angles; no effect larger than the expected statistical fluctuation was seen.

Errors on the beam position and size are found to have a negligible effect on the final result ($< 0.1\%$). The error due to the scaling factor k is taken into account in the statistical uncertainty on the decay length. Systematics errors are summarized in table 6.

Table 6: Systematic biases and uncertainties in the decay length analysis.

	$\Delta\tau_\tau/\tau_\tau$ (%)
Bias in Monte Carlo	-0.7 ± 1.3
$q\bar{q}$ background	-0.6 ± 0.3
Photon conversion	± 0.2
Beam size and position	negligible
Wrong track-hit assignment	± 0.6
Total	-1.3 ± 1.5

The total systematic bias and uncertainty is $-1.3 \pm 1.5\%$. The corrected τ lifetime obtained with the decay length method is

$$\tau_\tau = 298.0 \pm 10.6\,(\text{stat}) \pm 4.5\,(\text{syst})\,\text{fs}.$$

7 Conclusions

Three different techniques have been used to measure the τ lifetime from the 1991 ALEPH data sample. The newly-developed impact parameter sum method provides good statistical precision by virtually eliminating the impact parameter smearing due to the beam size in events of 1-1 topology. The impact parameter difference method yields small systematic errors because it requires no estimate of the τ production direction in the r-ϕ plane. The third measurement is obtained from three-prong decays by the conventional decay length method.

A weighted average of the three results is computed following the procedure described in [27]. The weights are determined from the uncertainties and correlations of the measurements. The correlation coefficient of the statistical errors from the two analyses of one-prong decays is determined from Monte Carlo simulation to be 0.22 ± 0.11. The common systematic errors are also accounted for. The combined result from the three techniques is

$$\tau_\tau = 295.5 \pm 5.9\,(\text{stat}) \pm 3.1\,(\text{syst})\,\text{fs},$$

where $m_\tau = 1777.1\,\text{MeV}/c^2$ has been assumed. The consistency of the three measurements is characterized by a χ^2 of 2.4 for two degrees of freedom (corresponding to a 30% probability).

The previous ALEPH measurements [13], adjusted[4] to correspond to the same m_τ, are combined with the present results in an analogous way, yielding

$$\tau_\tau = 294.7 \pm 5.4\,(\text{stat}) \pm 3.0\,(\text{syst})\,\text{fs}$$

with $\chi^2 = 3.6$ for six degrees of freedom.

Assuming e-μ universality, the ALEPH measurements [25] of $B(\tau \to e\overline{\nu}_e\nu_\tau)$ and $B(\tau \to \mu\overline{\nu}_\mu\nu_\tau)$ may be combined (with the appropriate phase space correction) to give an effective

[4]The relation between the mean decay length and the mean lifetime depends on m_τ. This relation is used in the impact parameter sum, impact parameter difference, and decay length methods, whereas the results of a conventional impact parameter analysis do not depend, to first order, on the assumed τ mass.

branching fraction $\bar{B}_e = 0.1794 \pm 0.0042$. With the ALEPH values of τ_τ and $\bar{B}_e$, the ratio of coupling constants from eq. 1 is $g_\tau/g_\mu = 0.997 \pm 0.016$. Using instead the world average $\bar{B}_e = 0.1799 \pm 0.0019$ [1], this ratio becomes $g_\tau/g_\mu = 0.998 \pm 0.012$. The present result is in excellent agreement with μ-τ universality.

8 Acknowledgements

We wish to thank our colleagues from the accelerator divisions for the operation of LEP. We are indebted to the engineers and technicians in all our institutions for their contribution to the good performance of ALEPH. Those of us from non-member countries thank CERN for its hospitality.

References

[1] K. Hikasa *et al.* (Particle Data Group), Phys. Rev. D **45** (1992) S1.

[2] E. Fernandez *et al.* (MAC Collaboration), Phys. Rev. Lett. **54** (1985) 1624.

[3] C. Bebek *et al.* (CLEO Collaboration), Phys. Rev. D **36** (1987) 690.

[4] H.R. Band *et al.* (MAC Collaboration), Phys. Rev. Lett. **59** (1987) 415.

[5] H. Albrecht *et al.* (ARGUS Collaboration), Phys. Lett. B **199** (1987) 580.

[6] M. Abachi *et al.* (HRS Collaboration), Phys. Rev. Lett. **59** (1987) 2519.

[7] W. Braunschweig *et al.* (TASSO Collaboration), Z. Phys. C **39** (1988) 331.

[8] D. Amidei *et al.* (MARK II Collaboration), Phys. Rev. D **37** (1988) 1750.

[9] C. Kleinwort *et al.* (JADE Collaboration), Z. Phys. C **42** (1989) 7.

[10] B. Adeva *et al.* (L3 Collaboration), Phys. Lett. B **265** (1991) 451.

[11] P. Abreu *et al.* (DELPHI Collaboration), Phys. Lett. B **267** (1991) 422.

[12] P.D. Acton *et al.* (OPAL Collaboration), Phys. Lett. B **273** (1991) 355.

[13] D. Decamp *et al.* (ALEPH Collaboration), Phys. Lett. B **279** (1992) 411.

[14] M. Battle *et al.* (CLEO Collaboration), Phys. Lett. B **291** (1992) 488.

[15] K. Riles, "Review of Tau Lepton Studies at LEP", University of Michigan, UM-HE-92-15, to appear in International Journal of Modern Physics, and references therein.

[16] J.Z. Bai *et al.* (BES Collaboration), SLAC-PUB-5870 and BEPC-EP-92-01 (1992).

[17] H. Albrecht *et al.* (ARGUS Collaboration), Phys. Lett. B **292** (1992) 221.

[18] D. Decamp *et al.* (ALEPH Collaboration), Nucl. Instrum. Methods A **294** (1990) 121.

[19] G. Batignani *et al.*, "Recent Results and Running Experience of the New ALEPH Vertex Detector", Conference Record of the 1991 IEEE Nuclear Science Symposium, 2–9 November 1991, Santa Fe, New Mexico, USA, Vol. 1, p. 438.

[20] "Alignment of the Aleph tracking devices", D. Decamp *et al.* (ALEPH Collaboration), Contribution to the 1992 Wire Chamber Conference, Vienna, 17–22 February 1992.

[21] D. Decamp *et al.* (ALEPH Collaboration), Phys. Lett. B **265** (1991) 430; Method A in photon identification section.

[22] D. Decamp *et al.* (ALEPH Collaboration), Phys. Lett. B **246** (1990) 306; the energy reconstruction algorithm.

[23] D. Decamp *et al.* (ALEPH Collaboration), Z. Phys. C **48** (1990) 365.

[24] Computer program KORALZ, version 3.8, courtesy of S. Jadach, B.F.L. Ward, and Z. Wąs; S. Jadach and Z. Wąs, Comp. Phys. Commun. **36** (1985) 191; Monte Carlo Group in "Proceedings of the Workshop on Z Physics at LEP", CERN Report 89-08 (1989) Vol. III; S. Jadach, B.F.L. Ward, and Z. Wąs, Comp. Phys. Commun. **66** (1991) 276.

[25] D. Decamp *et al.* (ALEPH Collaboration), Z. Phys. C **54** (1992) 211.

[26] Computer program KORALB; S. Jadach and Z. Wąs, Comp. Phys. Commun. **64** (1991) 267.

[27] L. Lyons, D. Gibaut, and P. Clifford, Nucl. Instrum. Methods A **270** (1988) 110.

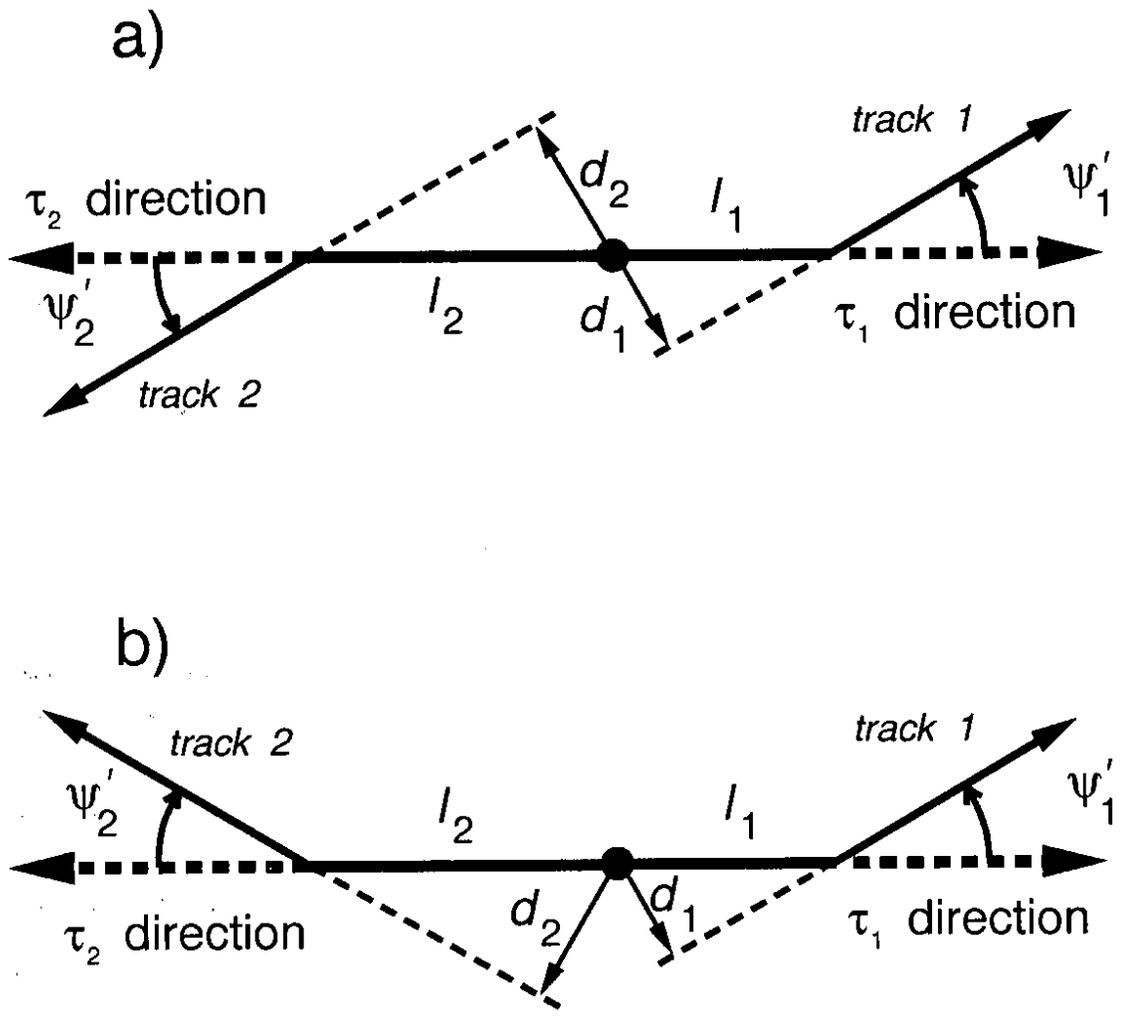

Figure 1: Decays with 1-1 topology: a) $\psi_1' > 0$, $\psi_2' > 0$; b) $\psi_1' > 0$, $\psi_2' < 0$. The positive z-axis points out of the page. Angles are measured counterclockwise.

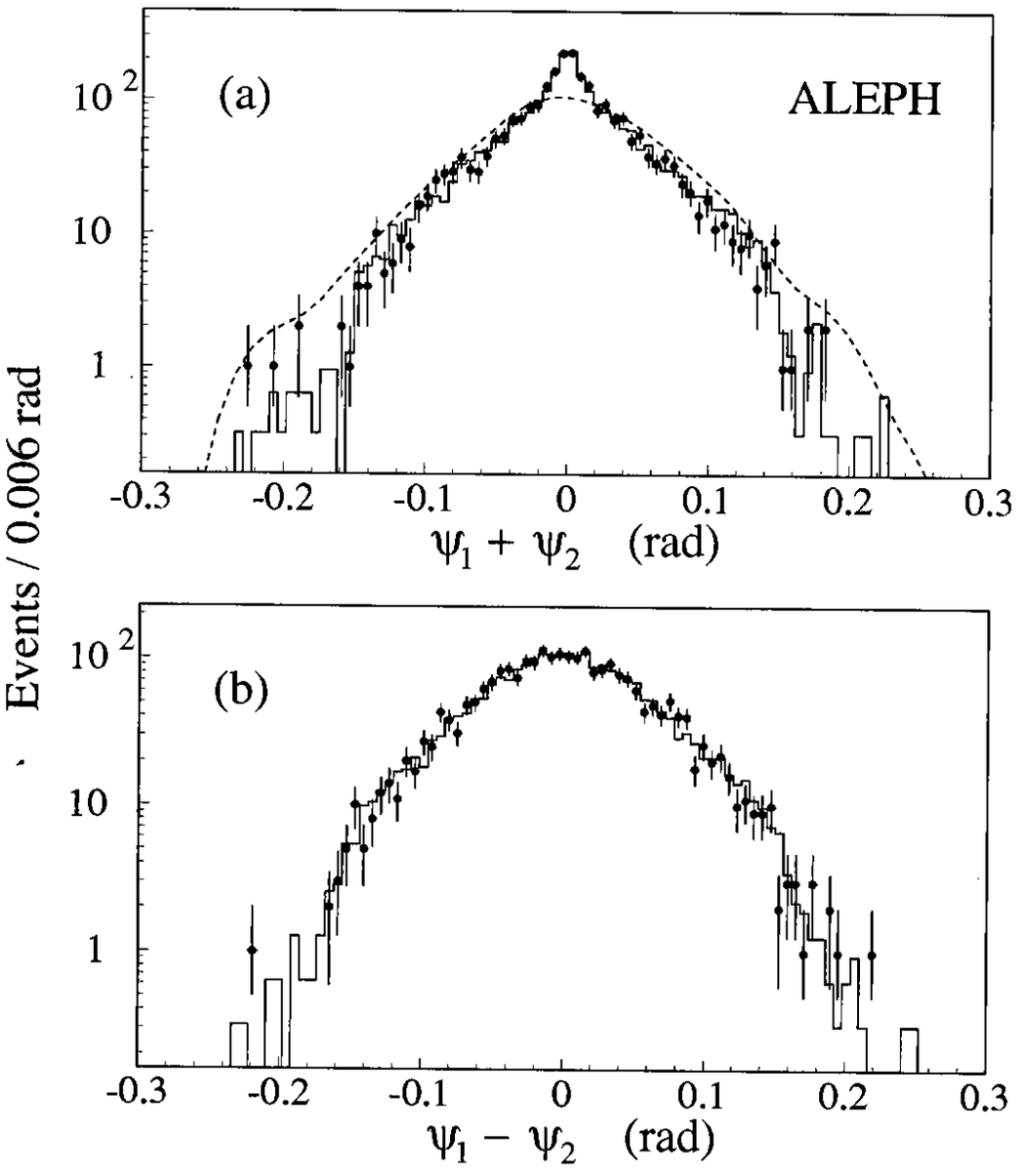

Figure 2: Distributions of (a) $S = \psi_1 + \psi_2$ and (b) $D = \psi_1 - \psi_2$ for τ Monte Carlo (histogram) and data (points). The dashed curve superimposed on (a) is the distribution of $S' = \psi'_1 + \psi'_2$ obtained from generated angles.

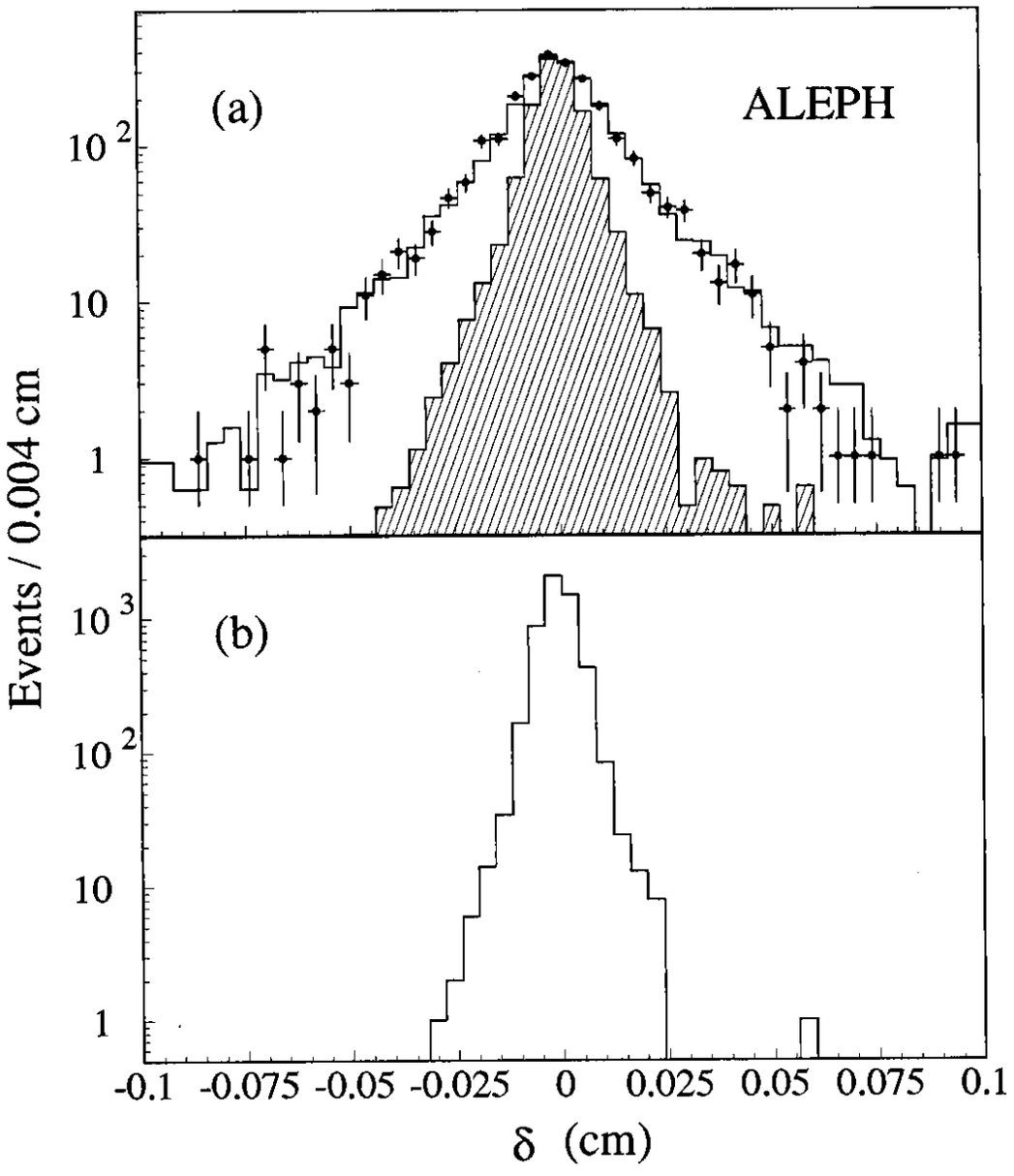

Figure 3: (a) Distribution of the sum of impact parameters δ for τ Monte Carlo (histogram), τ data (points) and zero-lifetime τ Monte Carlo (hatched histogram). (b) Same for dimuon data from Z decays.

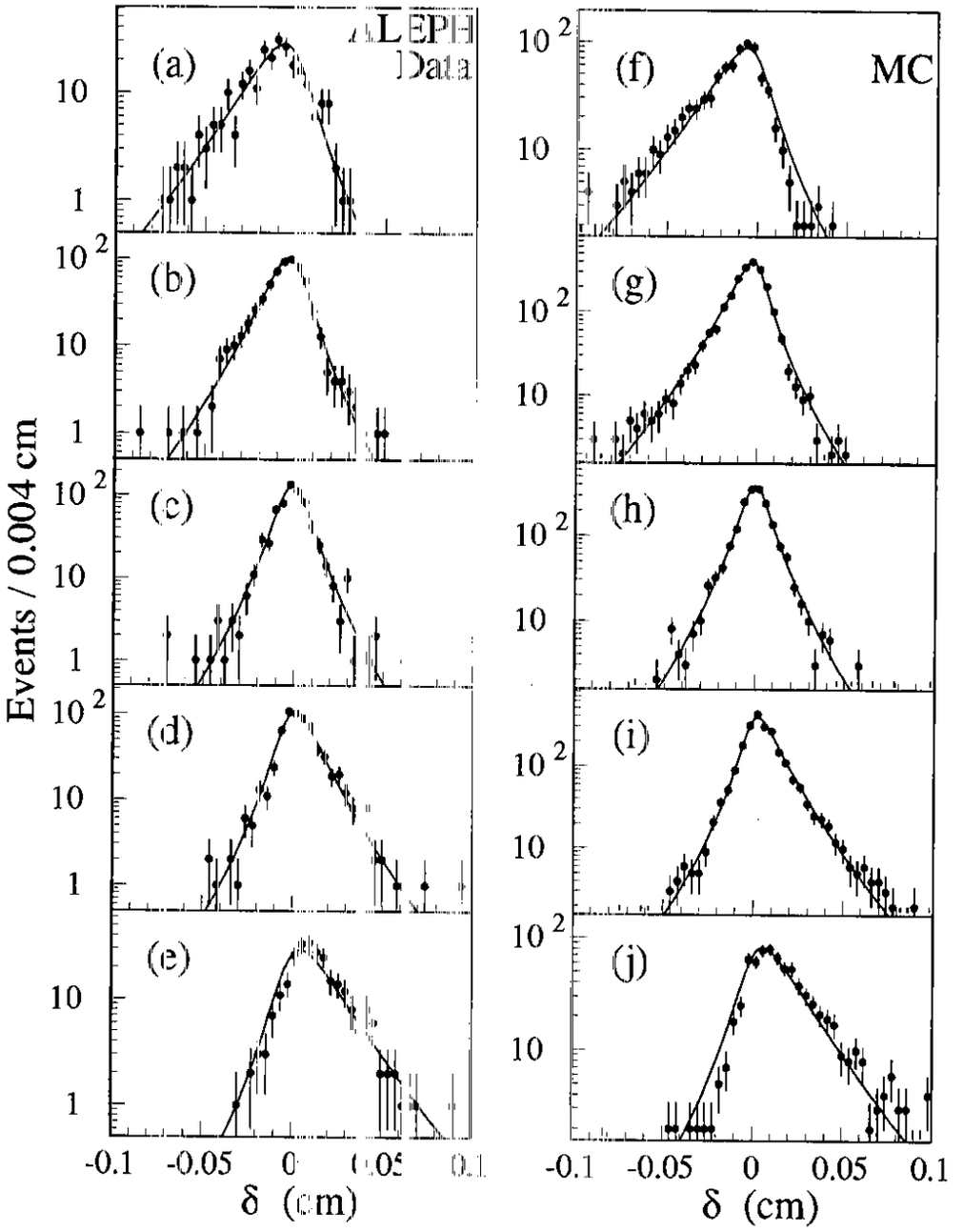

Figure 4: (a)-(e): δ distribution for various ranges of $S = \psi_1 + \psi_2$; (a) $S < -0.06$, (b) $-0.06 \leq S < -0.01$, (c) $-0.01 \leq S < 0.01$, (d) $0.01 \leq S < 0.06$, (e) $S \geq 0.06$. (f)-(j): same as (a)-(e) for simulated τ decays. The curves represent the fit result; systematic deviations from the real and simulated data are expected as mentioned in the text.

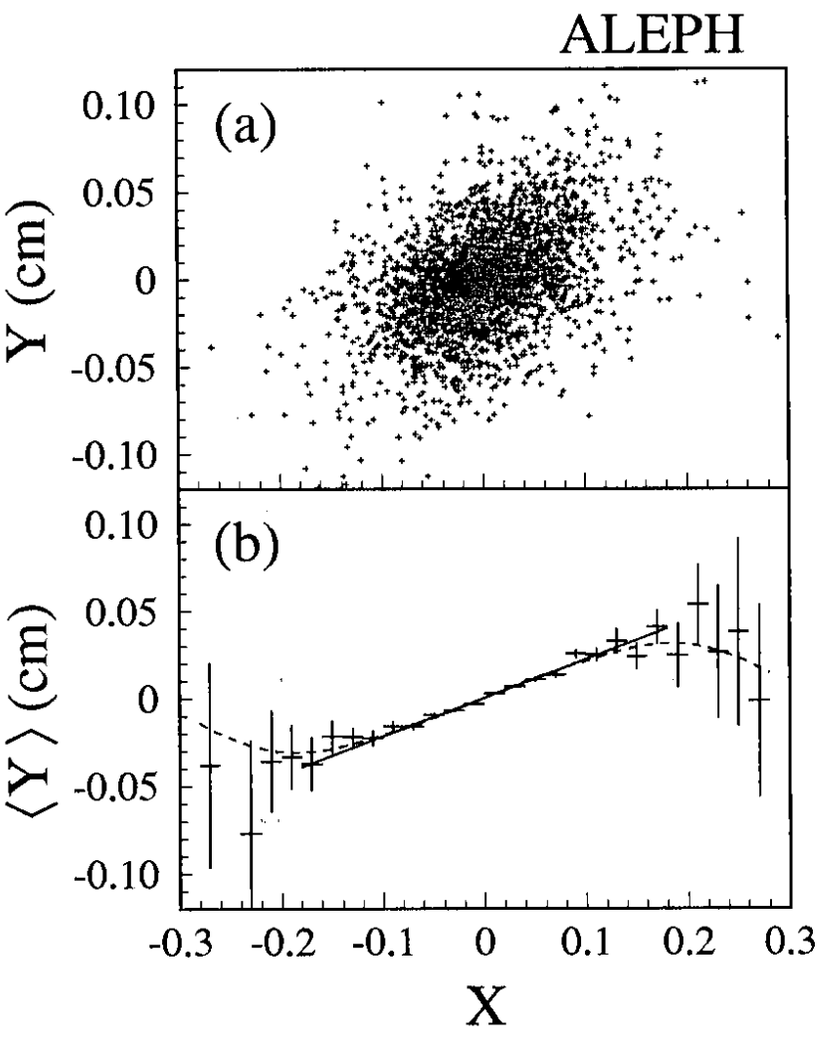

Figure 5: (a) Y *vs.* X for the accepted events. (b) $\langle Y \rangle$ *vs.* X for the data of (a). The line shows the result of the unbinned fit described in the text. The data are shown after trimming at $\pm 690\,\mu$m with respect to the best fit line. The dashed curve represents the expected behaviour from a Monte Carlo simulation of Z decays and two-photon interactions.

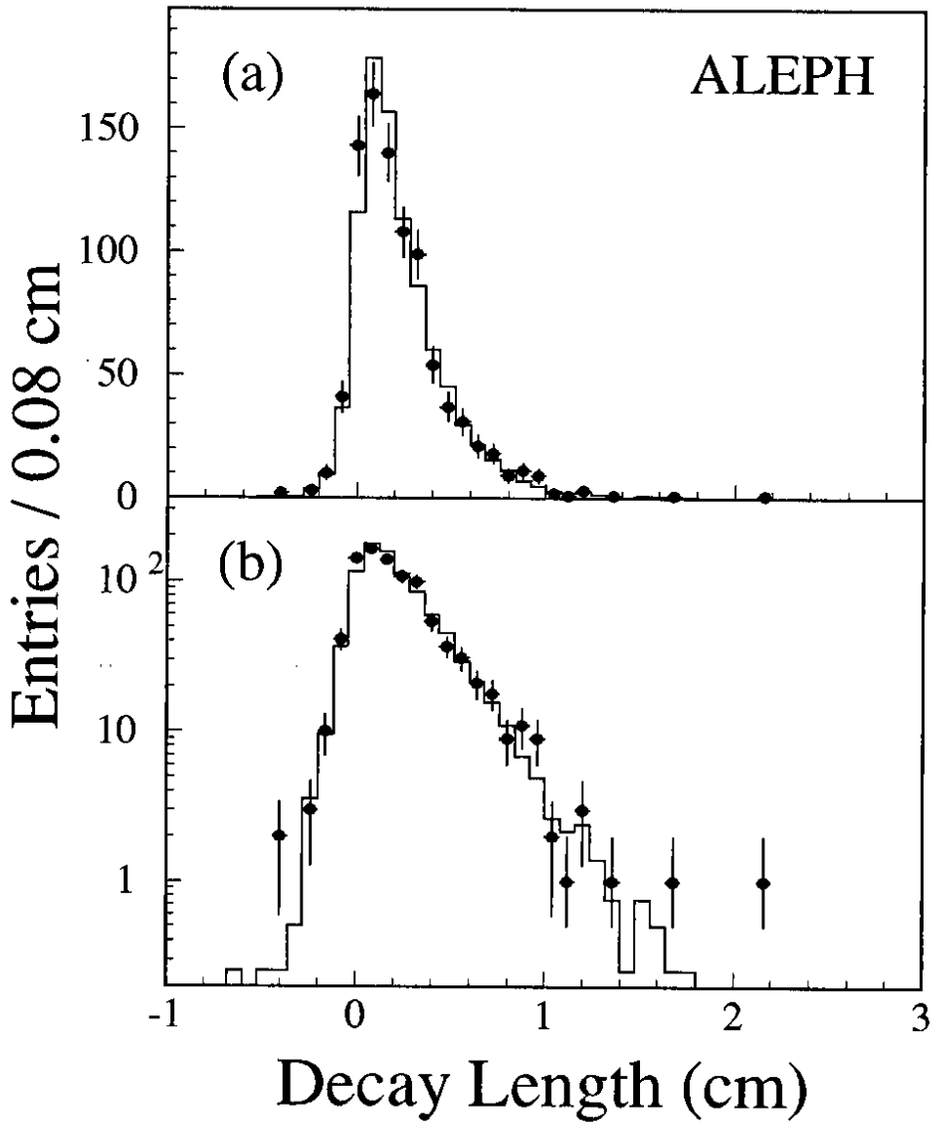

Figure 6: Decay length distribution for data (points) and Monte Carlo (histogram): (a) linear scale, (b) log scale. The generated τ lifetime is 304 fs.

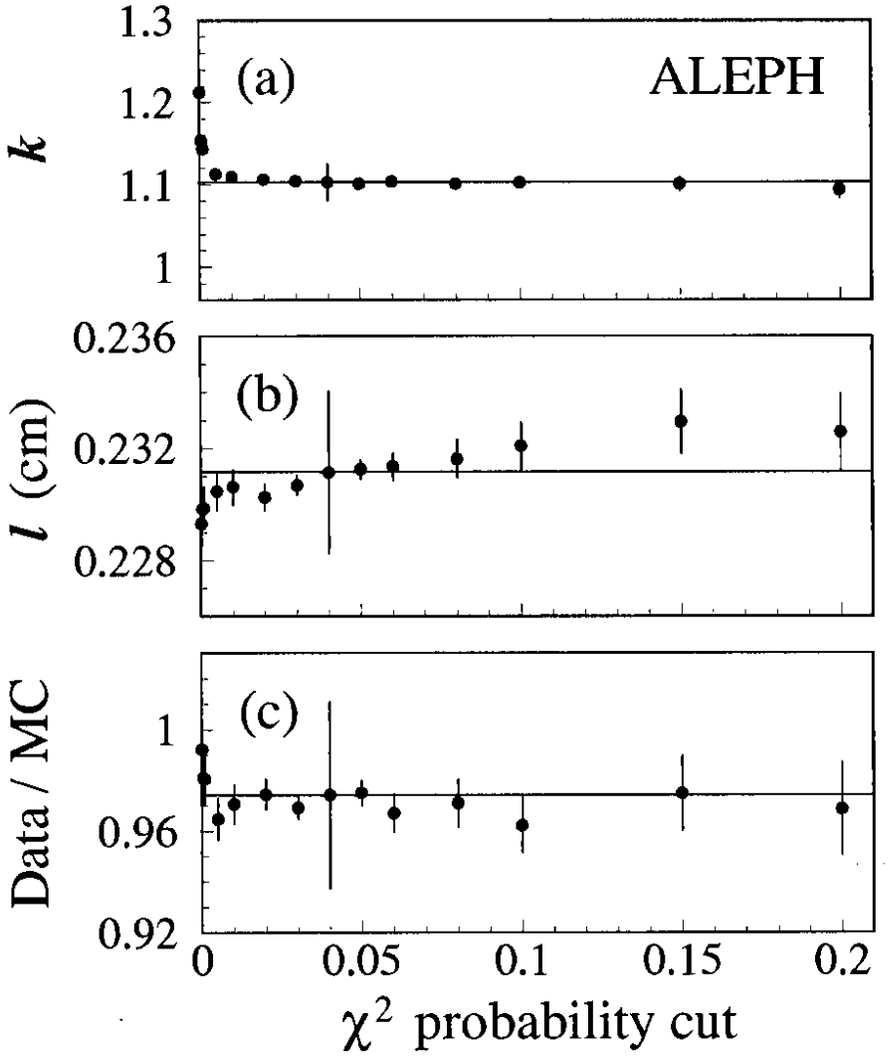

Figure 7: (a) Variation of k for Monte Carlo as function of the cut on vertex χ^2 probability. The error bar corresponding to the cut at 0.04 probability shows the total statistical error, while the other error bars are the expected variation from the reference point due to the different number of events. (b) Same for ℓ. (c) Ratio of data and Monte Carlo decay lengths.